Measurement 94 (2016) 12–18

Contents lists available at ScienceDirect

Measurement

journal homepage: www.elsevier.com/locate/measurement

Eliminating center discrepancies between simultaneously captured ILIDS and PIV images by means of direct homography estimation

Sebastian Kosch, Nasser Ashgriz *

Department of Industrial and Mechanical Engineering, University of Toronto, Canada

ARTICLE INFO

Article history:
Received 19 January 2015
Accepted 21 July 2016
Available online 22 July 2016

Keywords:
ILIDS
Droplet sizing
Spray characterization
Camera calibration
Center discrepancies
Image registration

ABSTRACT

Interferometric Laser Imaging for Droplet Sizing (ILIDS a.k.a. MSI or IPI) requires the objective lens to be defocused so that fringe patterns can be imaged. When two cameras are used (e.g. to perform simultaneous PIV and ILIDS measurements or to assist in the detection of overlapping droplet images) this defocusing introduces a distortion that thwarts an accurate calibration of the two cameras and makes a successful registration of the two images impossible. We show that to overcome the obvious difficulties presented by empirical ad-hoc estimates of this "center discrepancy" distortion, existing feature-based registration and/or point set registration algorithms can be used on the images to find the correct homography directly. This approach eliminates the need for camera calibration and leads to greatly improved matching between images.

1. Introduction

Interferometric Laser Imaging for Droplet Sizing (ILIDS), also known as IPI (Interferometric Particle Imaging) and MSI (Mie Scattering Imaging) is a popular optical droplet sizing method in which a spray is illuminated by a sheet of laser light and the scattered light is imaged laterally. The laser light is both reflected and refracted by the droplets, such that each droplet produces a pair of apparent "glare points". When seen through a lens away from the focal plane, each pair of glare points (the points being sources of coherent monochromatic light) appears as an interference pattern which, after falling through a circular aperture, casts an image that is a circular disk of fringes. The spatial frequency of the fringes is (to a very close approximation) linearly related to the droplet size. The phenomenon was first described by König et al. [15] and later in greater detail by Glover et al. [8]. Turnkey ILIDS setups for spray characterization are now widely available, comprising typically a pulsed Nd:YAG-laser, one or two CCD cameras, a timing circuit, and a piece of image processing software.

The ability to image a whole 2D field of droplets all at once is ILIDS' strongest selling point, yet also its curse. When droplets are spaced too closely, their defocused disk images overlap and it becomes difficult to determine the fringe counts corresponding to individual droplets. Damaschke et al. [5] provide a statistical estimate on the fraction of overlapping disks (overlap coefficient).

Arguably the most popular way to reduce the amount of overlap is the use of optical compression techniques, whether by means of a slit aperture [24] or a cylindrical lens [14,19]. However, some techniques (e.g. Global Phase-Doppler [6] and intensity-analyzing methods [25]) or use cases (e.g. very low signal-to-noise ratios) require the full disk image to be available. In these cases, the standard approach is to identify the location and outline of each disk image, such that the fringe analysis can either be limited to non-overlapping regions or be otherwise modified to take overlapping fringes into account.

1.1. Camera calibration and center discrepancies

Although a single camera is in theory sufficient to capture an ILIDS image, two cameras are often used in practice. One important reason is that a focused image, taken at the same instant as the defocused image, can provide a basis for the identification of overlapping disks mentioned above. This is the case, for instance, for the ILIDS system sold by Dantec Inc. Another reason for using two cameras can be the experimental requirement to perform two types of measurements simultaneously; examples of this are provided by Hardalupas et al. [9] (ILIDS and LIF) and Hardalupas et al. [10] (ILIDS and PIV).

To allow both cameras to image the same physical region in the spray, they are either placed behind a beam splitter at a right angle to the light sheet, or placed separately at different angles. The lat-

* Corresponding author.
E-mail addresses: skosch@mie.utoronto.ca (S. Kosch), ashgriz@mie.utoronto.ca (N. Ashgriz).

http://dx.doi.org/10.1016/j.measurement.2016.07.063
0263-2241/

ter approach makes for a more difficult setup, since Scheimpflug's rule demands that the camera must be tilted with respect to the objective lens, but it gives the user the freedom to choose the highest-intensity scattering angle.

In any of the above cases, the use of two cameras requires that their images be mapped onto one another. This is commonly achieved by means of a camera calibration procedure, in which a target pattern (e.g. as in Fig. 1) of known dimensions is photographed by each camera. A pattern recognition algorithm then determines the object-to-image mappings for each camera:

$$\begin{bmatrix} x' \\ y' \\ z' \\ r' \end{bmatrix} = \begin{bmatrix} S_x & A_{yx} & A_{zx} & T_x \\ A_{xy} & S_y & A_{zy} & T_y \\ A_{xz} & A_{xy} & S_z & T_z \\ P_x & P_y & P_z & S_0 \end{bmatrix} \begin{bmatrix} x \\ y \\ z \\ 1 \end{bmatrix}. \tag{1}$$

In practice, $P_{x,y,z} = 0$ and $S_0 = 1$ is assumed, such that the mapping is affine. The z-components (third row/column) are further assumed to be zero, such that a 3×3 matrix suffices for the purposes of this discussion:

$$\begin{bmatrix} x' \\ y' \\ r' \end{bmatrix} = \begin{bmatrix} S_x & A_{yx} & T_x \\ A_{xy} & S_y & T_y \\ P_x & P_y & S_0 \end{bmatrix} \begin{bmatrix} x \\ y \\ 1 \end{bmatrix}. \tag{2}$$

The camera calibration algorithm thus finds the camera matrices $\mathbf{P}_{\text{foc}}$ and $\mathbf{P}_{\text{def}}$ mapping the object coordinates $\mathbf{x}$ onto the two camera images $\mathbf{x}'_{\text{foc}}$ and $\mathbf{x}'_{\text{def}}$ (the respective subscripts shall hence designate the focused and defocused cameras):

$$\mathbf{x}'_{\text{foc}} = \mathbf{P}_{\text{foc}}\,\mathbf{x} \tag{3}$$

$$\mathbf{x}'_{\text{def}} = \mathbf{P}_{\text{def}}\,\mathbf{x}. \tag{4}$$

It follows that the quotient of the two matrices, also known as the homography

$$\mathbf{H} = \mathbf{P}_{\text{def}}\,\mathbf{P}_{\text{foc}}^{-1} \tag{5}$$

can be used to map the focused image onto the defocused image, as shown in Fig. 1:

$$\mathbf{H}\mathbf{x}'_{\text{foc}} = \mathbf{x}'_{\text{def}}. \tag{6}$$

Unfortunately, the camera calibration procedure itself introduces an unwanted distortion: to capture a viable photo of the target pattern, the defocused camera must be temporarily brought into focus, as was done in Fig. 1. However, as the camera is out of focus during the measurement process, both a blur and a scaling transformation are introduced. Fig. 2, adapted from Hardalupas et al. [10], shows schematically how this effect creates "center discrepancies". Since the extents of the defocused image are either smaller or larger than those of the focused image, depending on the direction of defocusing, all droplet images are projected either closer to or farther away from the image center. The discrepancy is worst for droplets far away from the image center. As a result, the centers of objects in simultaneously captured focused and defocused images no longer align (Fig. 3), and the camera calibration procedure becomes self-defeating.

While this error is easy to account for in the ideal case of right angles and perfect alignments (simply rescaling the image would solve the problem) the situation becomes more difficult in practice when the target pattern is no longer parallel to the camera sensor (intentionally or accidentally) or when cylindrical lenses are used to add optical compression. In fact, there is no guarantee that affine mappings are sufficient in the general case.

1.2. Context and structure of this paper

Surprisingly, only Hardalupas et al. [9,10] have hitherto published a discussion of this effect, and the only previous mention known to the authors is in Kurosawa et al. [16], who dismissed it as a "positioning error".

Hardalupas et al. identified the centers of particles in both PIV (focused) and ILIDS (defocused) images. They then empirically estimated the magnitude of the center discrepancy effect along the vertical axis, which enabled them to improve the accuracy of their nearest-neighbor-based droplet image matching algorithm.

In this article, we show that existing algorithms developed by the computer vision community in recent years can obviate the need for camera calibration entirely. Instead, we can use visual correspondences between the focused and defocused images to find the mapping between them directly. To that end, we first provide in Section 2 a brief overview over popular methods in the field of automated (linear) *registration*, i.e. the art of finding a *homography* (geometric mapping) between two *epipolar images* (images of the

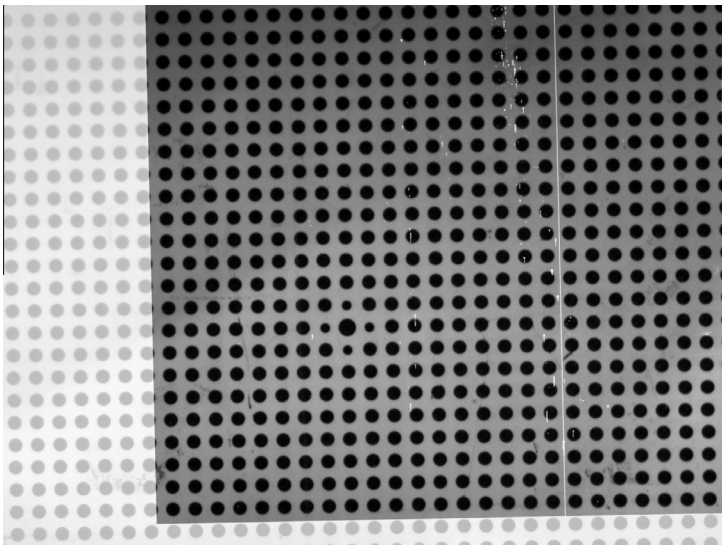

Fig. 1. Homography **H** applied to target pattern image captured by the focused camera and superimposed on the image captured by the defocused camera (here, both cameras were in focus for the calibration only).